Desalination and Water Treatment
www.deswater.com

doi: 10.5004/dwt.2017.21378

89 (2017) 304–314
September

Photocatalytic degradation of the antibiotic ciprofloxacin by ZnO nanoparticles immobilized on a glass plate

Majid Amiri Gharaghani[a,b], Mohammad Malakootian[a,b,*]

[a]*Environmental Health Engineering Research Center, Kerman University of Medical Sciences, Kerman, Iran, Tel. +98 343 132 5128, Fax: +98 343 132 5105; emails: m.malakootian@yahoo.com (M. Malakootian), amirimajid60@yahoo.com (M.A. Gharaghani)*
[b]*Department of Environmental Health, School of Public Health, Kerman University of Medical Sciences, Kerman, Iran*

Received 9 January 2017; Accepted 26 August 2017

ABSTRACT

Nano-photocatalysis is an advanced oxidation process used to degrade resistant organic compounds. This study was undertaken to investigate photocatalytic degradation of the antibiotic ciprofloxacin (CIP) by zinc oxide (ZnO) nanoparticles immobilized on a glass plate in aqueous solution. The resulting nanoparticles were characterized by X-ray powder diffraction (XRD), scanning electron microscopy (SEM) and pull-off adhesion testing. The parameters influencing removal that were investigated were pH, ZnO concentration, CIP concentration and contact time. Experiments were also conducted under optimal conditions on wastewater from a hospital in the city of Kerman. The results of XRD and SEM indicated that the ZnO immobilized on a glass plate was highly pure and uniform in size (60–70 nm). The results of the pull-off adhesion test was 4.1 MPa. Optimum conditions were pH: 11, reaction time: 90 min, ZnO concentration on the plate: 0.6 g/L and initial concentration of CIP: 3 mg/L. The maximum removal achieved was 98.36% and 90.25% for the synthetic solution and hospital wastewater, respectively. The photocatalytic degradation was linearly plotted and was found to follow pseudo-first-order degradation kinetics and was consistent with the Langmuir–Hinshelwood mode. The experimental data was analyzed using the Langmuir and Freundlich models of adsorption. The equilibrium data fitted well with the Freundlich model. Thermodynamic studies showed that adsorption was an exothermic process. Nano-photocatalysis using ZnO immobilized on a glass plate showed relatively high efficiency in removing ciprofloxacin from aqueous solutions and can be recommended for such purposes.

Keywords: Nano-photocatalytic; Ciprofloxacin; Zinc oxide; Immobilization; Glass

1. Introduction

Antibiotics enter the water and the environment through wastewater from residences, pharmaceutical industries, hospitals, veterinary clinics, agricultural production and fish farming pools [1,2]. One major group of antibiotics found in these environments is fluoroquinolones. Antibiotics well known in this class include ciprofloxacin (CIP), ofloxacin and norfloxacin. CIP is used globally for human and veterinary purposes [3].

The presence of CIP in wastewater and surface water, even in low concentrations, is an emerging environmental problem because of its continuous input and persistence in the aquatic ecosystem. Many studies have reported on the large number of pharmaceuticals in natural water and even in drinking water [3–5]; therefore, the removal of pharmaceuticals from aqueous solutions before entrance into the environmental cycle is crucial [6]. Biological degradation options for treating antibiotics have proven to be weak, but physiochemical processes such as advanced oxidation, ion exchange, adsorption on activated carbon and reverse osmosis can be used.

* Corresponding author.

Advanced oxidation processes (AOPs) are more effective and widely used for treating wastewater containing pharmaceuticals with the goal of complete removal of the contamination [7]. Photocatalytic oxidation is an AOP with powerful degradation ability against hydroxyl radicals for removing organic contaminants [8–10]. In photocatalytic degradation, the energy of light from ultraviolet (UV) rays or sunlight stimulates the surface electrons as photons when they come into contact with the catalyst atoms present in a sample [11]. These reactions are schematically shown in Fig. 1.

This stimulation causes excitation of the conduction band, resulting in movement of the electrons from the valence layer to the conduction band. The results of this change are generation of electron–hole pairs leading to development of free radicals as •OH or other radicals. The present compounds can be oxide organic materials [11]:

$$ZnO + h\upsilon \rightarrow e^- + h^+ \quad (1)$$

$$e^- + h^+ \rightarrow \text{heat} \quad (2)$$

$$h^+ + H_2O \rightarrow OH^\bullet + H^+ \quad (3)$$

$$h^+ + OH^- \rightarrow OH^\bullet \quad (4)$$

$$h^+ + CIP \rightarrow \text{Oxidation CIP} \quad (5)$$

$$e^- + O_2 \rightarrow O_2^{-\bullet} \quad (6)$$

$$O_2^{-\bullet} + HO_2^\bullet + H^+ \rightarrow H_2O_2 + O_2 \quad (7)$$

$$O_2^{-\bullet} + CIP \rightarrow CIP^{\bullet+} \quad (8)$$

$$OH^\bullet + CIP \rightarrow \text{Intermediate} \rightarrow CIP^{\bullet+} \quad (9)$$

Among different catalysts which can be used for photocatalysis, ZnO and TiO_2 have been more of interest than others. ZnO is more useful than TiO_2 because of its larger band gap and better stimulation by UV rays [12,13]. The application of nanosized catalysts for degradation of different contaminants brings about good adsorption results because ZnO nanoparticles offer attractive optical characteristics and a small size [14–16].

ZnO nanoparticles are toxic in suspension form; thus, for aqueous ecosystems [17], immobilization of nanoparticles on inert surfaces has been proposed [18,19]. Immobilization of ZnO nanoparticles on an inorganic plate can increase the catalyst lifetime in the reactor and has greater potential for reuse of the catalyst [19,20]. In previous studies, substrates such as quartz particles [21], chitosan grains [22] and silica gel granules [23] have been investigated.

Immobilization of nanoparticles on a glass plate prevents them from entering the aqueous environment [1]. The difficult recovery and UV light dispersion using nanoparticles in suspension form in photocatalytic processes can be solved by their immobilization on glass [19]. Furthermore, immobilization of ZnO nanoparticles on a glass plate can also improve their photocatalytic activity in comparison with that of suspended ZnO [18].

Darvishi Cheshmeh Soltani et al. [8] used photocatalysis with nanoparticles immobilized on a glass plate for degradation of formaldehyde in aqueous solutions. Akyol et al. [18] studied photocatalysis using ZnO nanoparticles for color removal. Malakootian et al. [24[, Malakootian and Hashemi Cholicheh [25], Malakootian et al. [26] employed nano-photocatalysis for removal of organic and inorganic contaminants. There have been no reports thus far on the use of ZnO nanoparticles immobilized on a glass surface as photocatalysts for the photocatalytic degradation of CIP in aqueous media. Considering the importance of subject, the current research was undertaken to study the efficiency of ZnO nanoparticles immobilized on a glass plate for degrading CIP in aqueous solution using UV rays.

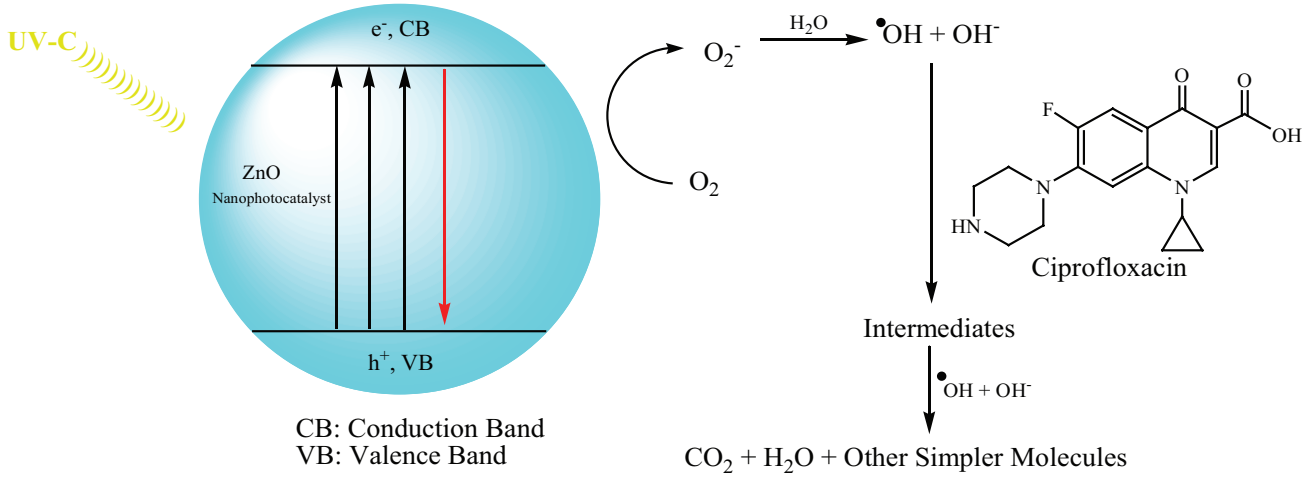

Fig. 1. Schematic diagram of mechanism of photocatalytic reaction taking place on the surface of ZnO nanoparticles immobilized on a glass plate.

2. Method

2.1. Materials

CIP with a purity of 99% was purchased from Tamad Pharmaceuticals (Tehran, Iran). The ZnO nanoparticles (average particle size 60–72 nm; specific surface area = 15–25 m^2/g) of experimental purity were purchased from Sigma-Aldrich (USA) and used without further purification. ZnO nanoparticles were supplied in white powdered form. Sulfuric acid and sodium hydroxide of experimental purity were supplied by Merck (Germany). H_2SO_4 and NaOH 0.1 N solutions were used to adjust the pH where necessary.

2.2. Immobilization of ZnO nanoparticles on glass plates

Different concentrations of ZnO nanoparticles were prepared in double-distilled water. This mixture was then placed on a magnetic stirrer for 1 h at 300 rpm. Thereafter, it was heated at 50°C for 90 min in an ultrasonic device to obtain a completely homogeneous suspension [8,20,27]. Three glass plates with dimensions of 20 × 3 cm were used as beds on which to immobilize the ZnO nanoparticles. The surfaces of these plates were sandblasted to improve adhesion of the ZnO nanoparticles. Next, to activate the surface of the glasses for better immobilization, they were placed in concentrated NaOH for 24 h. After removal of the glass plates from NaOH, they were washed with deionized water several times until the pH of the rinse water reached a value of about 7 [20,27]. In the next stage, the suspension was uniformly coated onto the glass surface and dried at room temperature for 24 h. For calcination of the coated glass plates, they were placed inside a furnace at 450°C for 3 h [8,20,27]. The plates were thoroughly washed with deionized water before testing for removal of all unattached ZnO nanoparticles.

2.3. Photodegradation experiments

Direct photolysis (without catalyst) of the CIP was determined in the same reactor under similar conditions. The pollutant removal efficiency of the UV/ZnO process was subtracted from the removal efficiency of direct photolysis (CIP degradation by UV light alone) and experiments in the dark. This obtained the synergetic effects of the process and the percentage of adsorption by ZnO at different concentrations of CIP.

The experiments were performed using techniques set forth in the Standard Methods for the Examination of Water and Wastewater (20th edn.) [28]. The effect of CIP concentration (3, 5, 7 and 9 mg/L), pH value (3, 5, 7, 9 and 11), nanocatalyst concentration (0.6, 1 and 1.4 g/L) and exposure time (15, 30, 45, 60, 75 and 90 min) to a UV-C lamp with a peak intensity of 254 nm (Philips, The Netherlands) 2 cm above the surface of the glass plate on the removal efficiency of the antibiotic was investigated. Over the course of the research, the parameters of interest were optimized. After reaching optimal conditions, the experiment was performed on a sample of hospital wastewater from the city of Kerman in southeastern Iran. The physical and chemical characteristics of the hospital wastewater are shown in Table 4. All experiments were performed at room temperature (25°C ± 1°C). The removal efficiency of CIP from the synthetic and real solutions was calculated as:

$$E = \frac{(C_0 - C_t)}{C_0} \times 100 \tag{10}$$

where E is the removal efficiency (%) and C_0 and C_e are the initial and equilibrium concentrations of CIP (mg/L), respectively.

The kinetic degradation data were analyzed using the Langmuir–Hinshelwood (L–H) and pseudo-first-order kinetic models. The Freundlich and Langmuir isotherm linear models (without UV light) were used for assessing the adsorption equilibrium data. The amount of drug adsorbed onto the adsorbent was calculated as:

$$q_e = \frac{(C_0 - C_e)V}{m} \tag{11}$$

where q_e is the amount of equilibrium adsorption (mg/m^2), V is the solution volume (L) and m is the amount of adsorbent employed (g).

2.4. Photoreactor

A reactor was designed and used for testing as shown in Fig. 2 [8]. A cuboid experimental reactor made of Plexiglass 25 cm in length, 10 cm in width and 5 cm in height was used for photocatalytic degradation of CIP in an aqueous phase. The volume of the exploitable container was 750 cc. Three 6 W low pressure UV-C lamps (Philips) were deployed at the top of the reactor. The reactor was designed such that the distance between the catalyst surface and the radiation source was minimized to increase production of hydroxyl radicals through stimulation of the catalyst. For reactor mixing, a peristaltic pump was used with a flow rate of 1 mL/s [8,20].

2.5. Analysis

The pH of the solution was measured by a pH meter (Hanna Instruments, Japan). A UV spectrophotometer (Shimadzu, Japan) was used to measure the CIP concentration in solution at λ_{max} = 276 nm. An ultrasonic device was employed to synthesize the homogeneous suspension and a digital balance (Shimadzu, Japan) to weigh the materials.

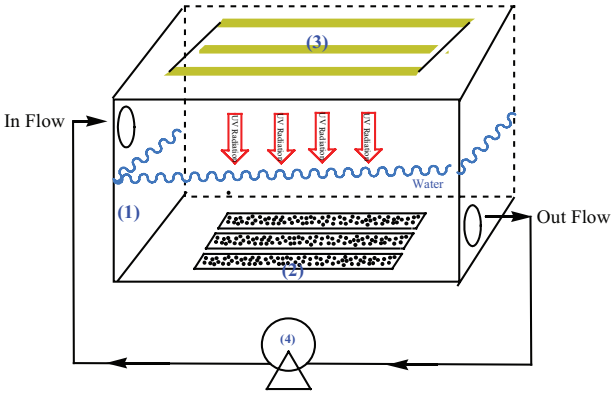

Fig. 2. The system used for performing the nano-photocatalytic process ((1) the reactor made of Plexiglass, (2) ZnO nanoparticles immobilized on glass, (3) UV lamp, (4) the peristaltic pump).

A furnace was used for calcination of the glass. Determination of the structural characteristics of the immobilized catalyst (constituent phases and crystal size of nanoparticles) was done by X-ray powder diffraction (XRD) (GNR, MP 3000, Italy). Analysis of the results was reported in SPSS 22 through descriptive statistics.

The efficiency of photocatalytic degradation in real wastewater containing CIP was carried out using a Knauer Smart line HPLC (C8 column; 250 × 4.6 × 5 mm; Knauer-D-14163 Berlin, Germany) with a UV detector at a wavelength of 272 nm. The mobile phase was a mixture of 10 μm HCl and acetonitrile at a ratio of 80/20 (vol%) with an injection flow rate of 1 mL/min. Scanning electron microscopy (SEM) (MIRAG TESCAN, Czech Republic) was performed to detect the morphology of the ZnO nanoparticles immobilized on glass plates. Adhesion testing was done using an Elcometer (model 108) at 25°C with 30% humidity (ASTM D 4541-09).

3. Results and discussion

3.1. XRD analysis of ZnO nanoparticles immobilized on a glass plate

Fig. 3 shows the XRD results of the chemical structure of the ZnO nanoparticles immobilized on a glass plate. The peaks represent the hexagonal structure of the ZnO and are congruent with the standard spectra of the device (Joint Committee Powder Diffraction Standards; JCPDS card 05-0664). The XRD spectra do not show extra peaks denoting other elements. The XRD patterns indicate the crystal nature of the ZnO with a crystal phase that is hexagonal (Wurtzite) with no impurities.

3.2. SEM analysis of ZnO nanoparticle immobilized on glass plate

The surface morphology of the immobilized ZnO nanoparticles was analyzed by SEM and the results are shown in Fig. 4. The figure shows that, after immobilization of the nanoparticles on glass, their porosity remained within desirable limits and their size was consistent. The SEM images clearly show spherical ZnO nanoparticles of 60–72 nm in size.

3.3. Pull-off adhesion test

Pull-off adhesion testing of the immobilized ZnO nanoparticles on glass plates showed a pull-off strength of more than 4.1 MPa.

3.4. Comparison of processes involved in photocatalysis

Before evaluation of the effect of operational parameters influencing photocatalytic degradation of CIP, the roles of adsorption, photolysis and photocatalysis were determined separately to achieve a better understanding of the efficiency of the photocatalytic process itself. The results show a slight contribution of adsorption and photolysis using UV lamps alone for the removal of CIP at removal rates of 4.8% and 15.9%, respectively, in 90 min. A short reaction time of 90 min was sufficient for photocatalysis using immobilized ZnO nanoparticles to degrade 74.52% of CIP in aqueous solution (Fig. 5).

The results indicate that ZnO shows insignificant photocatalytic activity under visible light irradiation because the band gap of ZnO (3.27 eV) is available only under UV radiation and is not provided by the visible light radiation used here. UV light provides a higher intensity (lower wavelength or higher energy), allowing the light to easily penetrate and form more hydroxyl radicals, which increases the rate of photocatalytic degradation of CIP [29]. Shafaei et al. [30] studied photocatalytic degradation of terephthalic acid using titania and zinc oxide photocatalysts. They observed that UV light alone was not efficient enough to degrade

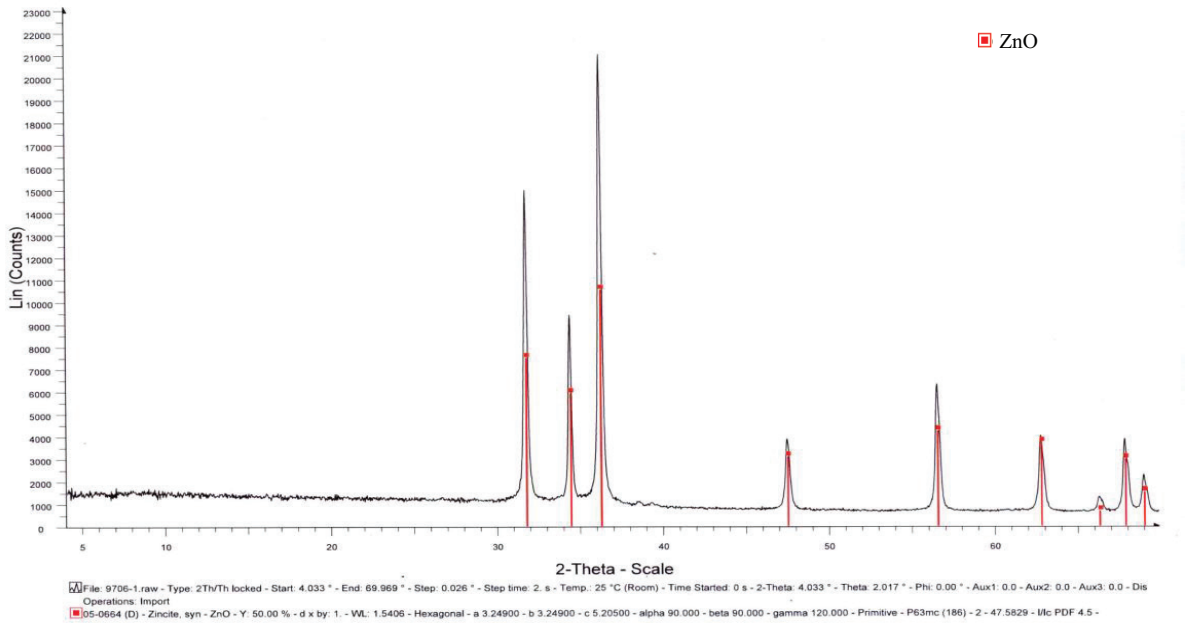

Fig. 3. XRD pattern of ZnO nanoparticles immobilized on glass plate.

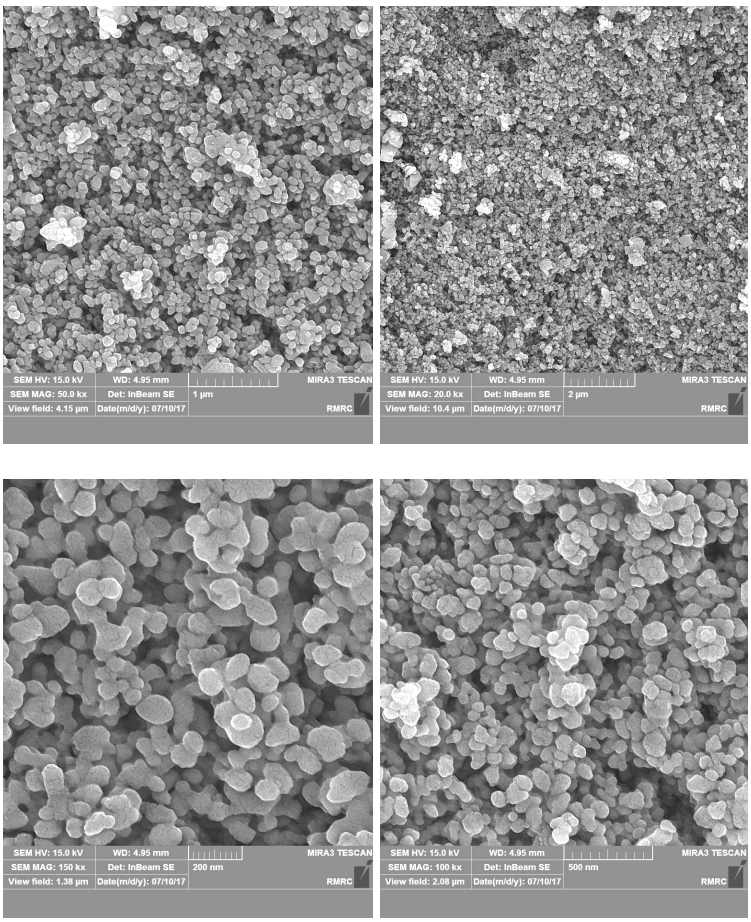

Fig. 4. SEM images of ZnO nanoparticles immobilized on glass plate.

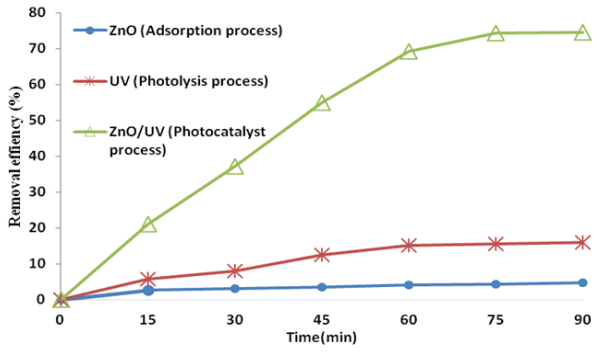

Fig. 5. Removal efficiency of different processes involved in photocatalytic degradation of CIP (initial CIP concentration = 3 mg/L, initial pH = 7, dose of ZnO = 0.6 g/L, distance between UV and ZnO = 2 cm).

terephthalic acid, but the addition of a photocatalyst accelerated the photodegradation.

3.5. Effect of initial pH

The results of the effect of pH vs. time are shown in Fig. 6. As seen, an increase in pH from 3 to 11 at a concentration of 3 mg/L of CIP and 0.6 g/L of immobilized ZnO increased the removal from 23.54% to 84.6%. The optimal pH was thus selected to be 11 and the following stages of testing were conducted at this optimal pH.

The pH of the solution is an important parameter in photocatalytic reactions. Variations in pH affect the superficial charge of the catalyst and influence the degree of ionization and isolation of functional groups at active sites on the catalyst. They also affect the chemistry of the solution [30]. The basis of their activity is generation of hydroxyl radicals. Maximum removal efficiency took place at a pH of 11. The reason for the increase in efficiency at this pH is that the level of OH^- increased. Upon UV radiation of the catalyst surface, holes developed (h^+_{VB}) as shown in Eqs. (1) and (4) that generated hydroxyl radicals having high oxidation abilities that enhanced the photodegradation rate of CIP.

At low pH values, the high concentration of protons (H^+), which have high continuity with hydroxyl anions, inhibited formation of hydroxyl radicals. Maximum antibiotic stability takes place in acidic pH because the carboxyl group (COOH) is not ionized [11]. CIP is an ampholytic compound with a pK_a value of 8.74 for the nitrogen on the piperazinyl ring and 6.09 for the carboxylic group. The isoelectric point of zwitterions occurs at a pH of 7.4. CIP appears to be most sensitive to photodegradation in zwitterionic form at a slightly basic pH [31]. Avisar et al. [32] studied removal of CIP by UV.

They observed that an increase in pH increased the rate of removal of CIP. El-Kemary et al. [11] examined photocatalytic degradation of CIP and reported maximum removal at pH values of 7–10, which is congruent with the results of the current research.

3.6. Effect of catalyst concentration

Fig. 7 shows that an increase in the concentration of ZnO immobilized on glass decreased the process efficiency. An increase in the ZnO concentration decreased the extent of removal from 75% to 60%. The optimal percentage of catalyst was determined to be 0.6 g/L for a removal efficiency of 75%.

The concentration of the photocatalyst is a critical parameter in photocatalytic oxidation. In this study, the ZnO concentrations investigated were 0.6, 1 and 1.4 g/L. In the absence of ZnO, degradation did not occur, which indicates that CIP cannot be degraded by photolysis only [8]. On the other hand, the rate of reaction was found to decrease as the ZnO concentration increased. An increase in ZnO was expected to increase the number of active sites available for CIP adsorption and the total surface area exposed to light, increasing the number of free radicals generated and causing the removal rate to rise [33]. However, as the concentration of catalyst per unit area (of glass) increased, the nanoparticles agglomerated, decreasing the availability of active sites and reducing the removal efficiency. Indeed, a high dose of ZnO catalyst caused overlapping of the catalyst surface and their agglomeration. This diminished the total area available and the level of degradation of the contaminant [34].

Immobilized semiconductor systems also suffer from mass transfer limitations caused by the decrease in specific surface when compared with traditional systems [35]. Bekkouch et al. [36] studied the effect of adsorbent concentration on the adsorption of phenol by TiO_2 and reported similar results. They reported that an increase in the nanoparticle concentration above the equilibrium level caused them to agglomerate and the percentage of adsorption efficiency remained constant. Wang et al. [37] concluded that an increase in the amount of montmorillonite adsorbent increased the removal efficiency of CIP. The reason for the increase in efficiency was an increase in the number of active adsorption sites. Behnajady et al. [19] increased the photoactivity of titanium dioxide immobilized on a glass plate by optimizing the heat attachment method parameters. They reported that an increase in the concentration of TiO_2 slurry decreased the photoactivity of TiO_2 immobilized on glass plates. This was caused by the agglomeration of TiO_2 particles at high concentrations of TiO_2.

3.7. Effect of initial CIP concentration

Fig. 8 shows the results of the investigation of the effect of initial concentration of CIP vs. time. In terms of the effect of the initial concentration of the CIP and determination of the optimal concentration on the efficiency of the process, an increase in the initial concentration decreased the removal efficiency. A concentration of 3 mg/L of CIP produced the maximum removal efficiency of the antibiotic. With an increase in the concentration of CIP to 9 mg/L, the efficiency of CIP removal decreased.

The results of the effect of the initial concentration of CIP on the removal efficiency indicate that an increase in initial concentration decreased the removal efficiency. For certain periods of time and concentrations of ZnO and at

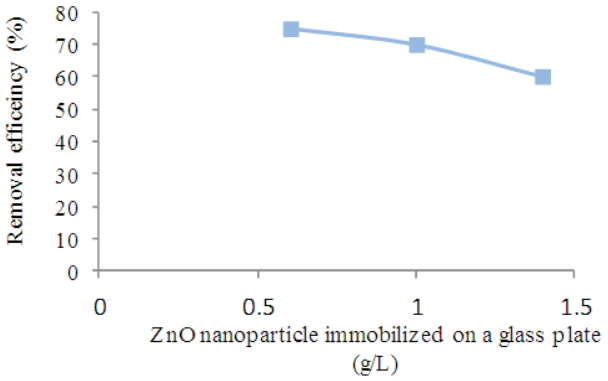

Fig. 7. Effect of dose of ZnO on removal of the antibiotic CIP from aqueous solutions (CIP concentration = 3 mg/L, contact time = 60 min, pH = 11, distance between UV and ZnO = 2 cm).

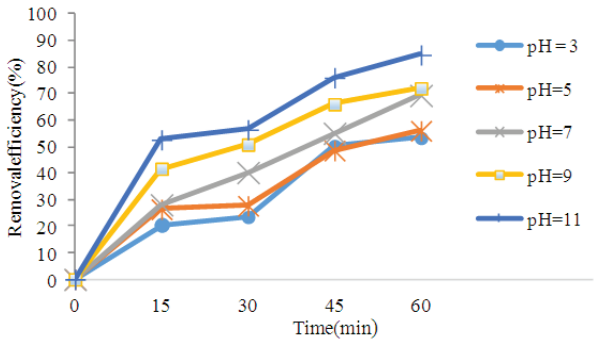

Fig. 6. The effect of pH in removing the antibiotic CIP across different times (initial concentration = 3 mg/L, dose of ZnO = 0.6 g/L, distance between UV and ZnO = 2 cm).

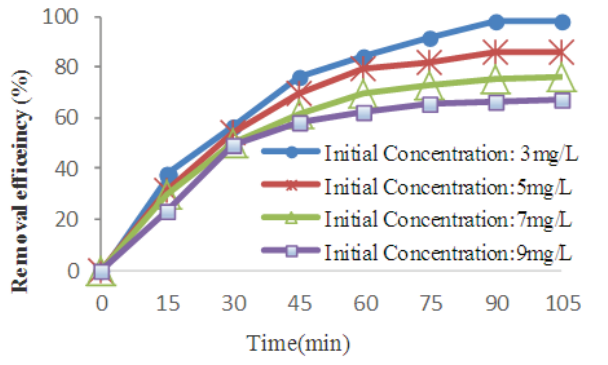

Fig. 8. Effect of the initial concentration of the antibiotic on the degree of removal (contact time = 105 min, pH = 11, dose of ZnO = 0.6 g/L, distance between UV and ZnO = 2 cm).

a constant pH, an increase in the concentration decreased the removal efficiency. The maximum removal efficiency (98.36%) related to an initial concentration of 3 mg/L that occurred after 105 min of reaction time.

The descending trend in removal efficiency with an increase in initial concentration occurs because, at a constant level of ZnO, the active sites on the catalyst are fixed. With the increase in the concentration of CIP, the mol rate of contaminant increases for the reaction medium and the active sites become saturated, thus reducing the removal efficiency [29]. This can also be attributed to the increase in the driving force of the concentration gradient in response to the increase in initial concentration of the molecules present in the solution [38]. Jiang et al. [39] studied adsorption of CIP using biomass. They observed that an increase in the initial concentration of CIP decreased the removal efficiency. Zhao et al. [40] studied the removal of tetracycline and observed that an increase in the initial concentration of tetracycline decreased the removal efficiency, which is congruent with the results of the current research.

3.8. Effect of reaction time

The results obtained from the effect of time on removal of the CIP are shown in Fig. 9. The figure shows the percentage of degradation of CIP by ZnO nanoparticles vs. the irradiation time. The results indicate that an increase in contact time decreased the amount of CIP remaining in solution. The removal percentage reached a maximum at 105 min and afterward the process efficiency reached near-equilibrium state.

Exposure time is another influential parameter for determination of process performance. The results indicate that an increase in reaction time to 90 min resulted in a significant removal efficiency of about 98.36%. Increasing the removal efficiency of CIP by increasing the reaction time could be attributed to an increase in OH^- generated as the process continued [34]. On the other hand, further collision of UV rays with the surface of ZnO catalyst liberated the electron–hole pairs, resulting in further production of hydroxyl radicals [41]. Safari et al. [42] concluded that an increase in the reaction time increased removal efficiency. They considered a reaction time of 90 min to be the equilibrium time, which is similar to the results of the current study. Zhang et al. [43] studied adsorption of CIP and determined an equilibrium time of 100 min, after which adsorption continued slowly.

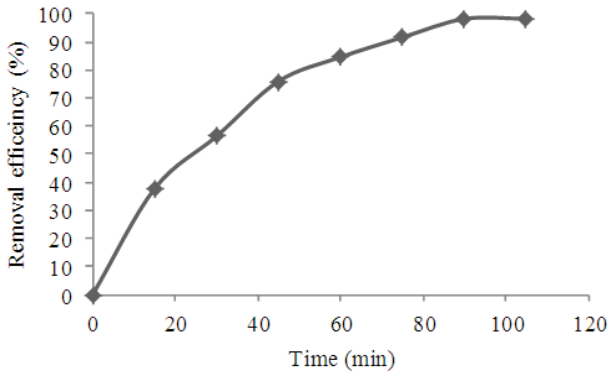

Fig. 9. Effect of contact time on the removal of the antibiotic CIP (initial concentration = 3 mg/L, pH = 11, dose of ZnO = 0.6 g/L, distance between UV and ZnO = 2 cm).

3.9. Isothermal study of CIP photocatalytic degradation

Isothermal studies were carried out at different concentrations of CIP in the solution (1–10 mg/L) with 0.6 g/L of the adsorbent immobilized on glass for an equilibrium time of 35 min at 25°C (without UV light). Linear models of the Langmuir and Freundlich isotherms were used to fit the adsorption equilibrium data as shown in Eqs. (12) and (13), respectively. The linear form of the Langmuir isotherm is:

$$\frac{C_e}{q_e} = \frac{1}{bq_m} + \frac{C_e}{q_m} \tag{12}$$

where q_m is the maximum adsorption capacity of the adsorbent (mg/g) and b is the Langmuir adsorption constant (L/mg). The linear form of the Freundlich isotherm is:

$$\ln q_e = \ln K_F + \frac{1}{n}\ln C \tag{13}$$

where n and K_F are Freundlich constants related to the intensity of the adsorbent and its capacity, respectively [44–46].

Fig. 10 shows the Langmuir isotherm curve and Fig. 11 shows Freundlich isotherm curve. The parameters of Langmuir and Freundlich equations are listed in Table 1. The correlation coefficient between the experimental data and adsorption isotherms was greater for the Freundlich than the Langmuir isotherm, suggesting that the Freundlich isotherm better predicts the process of adsorption of CIP onto ZnO adsorbent.

Adsorption isotherms explain the behavior of the reaction between the adsorbate and adsorbent. The most important pattern of adsorption is stated through the isotherm [44]. The results of this study indicate that the R^2 (correlation coefficient) values for the Langmuir and Freundlich isotherms were 0.91 and 0.95, respectively; therefore, the Freundlich isotherm is preferable for explaining the adsorption of CIP.

The regions available on the surface of the adsorbent were not uniform and were multilayered [47]. Whenever the value of $1/n$ is greater than 1, adsorption is physical, otherwise it

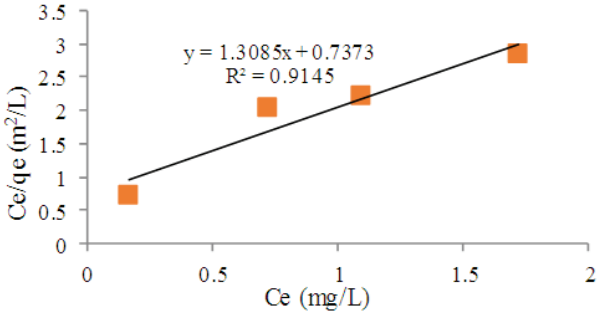

Fig. 10. The Langmuir isotherm curve.

will be chemical [48]. The value of n in this study was 0.40, suggesting that the adsorption was chemical. Chen et al. [49] indicated that the process of adsorption of CIP is in better accord with the Freundlich isotherm. On the other hand, Shafey et al. [50] investigated the adsorption isotherms for CIP and concluded that adsorption is more in line with the Langmuir isotherm.

3.10. Kinetics of CIP photocatalytic degradation

To investigate the kinetics of the process of photodegradation of CIP by ZnO, the pseudo-first-order and Langmuir–Hinshelwood models were used. The degradation experiments using UV irradiation of CIP aqueous solutions containing ZnO followed pseudo-first-order kinetics with respect to the concentration of CIP in the bulk solution:

$$\mathrm{Ln}(C_t/C_0) = -K_{obs}\,t \tag{14}$$

A graph was plotted for $\mathrm{Ln}C_0/C_t$ as a function of time (t) where C_0 is the initial concentration of CIP and C_t is the concentration of CIP at time t. From the slope of the plot, the rate of photocatalytic degradation of CIP was determined. K_{obs} is the apparent pseudo-first-order rate constant and is affected by CIP concentration.

L–H kinetics better explains heterogeneous photocatalytic degradation to determine the relationship between the initial degradation rate and the initial concentration of organic substrate. This mechanism proposes that both adsorbing and adsorbed molecules undergo a bimolecular reaction, in this case, hydroxyl radicals and CIP. The L-H expression that explains the kinetics of heterogeneous catalytic systems is:

$$\frac{1}{K_{obs}} = \frac{1}{K_C K_{L-H}} + \frac{C_0}{K_C} \tag{15}$$

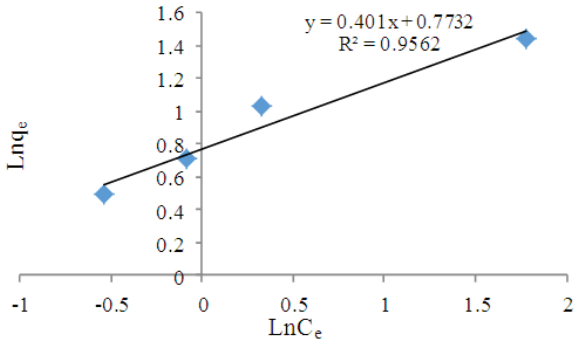

Fig. 11. The Freundlich isotherm curve.

Table 1
The parameters of Langmuir and Freundlich models for adsorption of CIP by ZnO adsorbent

Freundlich model			Langmuir model		
R^2	K_F (mmol/g)	$1/n$ (L/g)	R^2	b (L/mg)	Q_m (mg/g)
0.95	2.17	0.40	0.91	1.78	0.76

where C_0 is the initial concentration of CIP (mg/L), $K_{L\text{-}H}$ is the L-H adsorption equilibrium constant (L/mg) and K_c is the rate constant of surface reaction (mg/L min). K_{obs} can be obtained directly from regression analysis of the linear curve in the plot [51,52]. The values which correspond to different initial concentrations, along with the regression coefficients, are listed in Table 2.

Plotting $1/K_{obs}$ against C_0 (Fig. 12) shows a straight line with $R^2 = 0.9953$, which reveals that adsorption is involved in photodegradation. The calculated adsorption coefficient and constant equilibrium for the L-H model were 0.245 mg/L min and 0.158 L/mg, respectively.

One of the most important factors in the design of a photodegradation system for determination of the optimal contact time is prediction of the degradation rate controlled by kinetics [53,54]. Photocatalytic degradation was linearly plotted according to pseudo-first-order degradation kinetics and was consistent with the L-H model. The correlation constants for the fitted line were calculated to be $R^2 = 0.951$, 0.946, 0.977 and 0.994 for CIP concentrations of 3, 5, 7 and 9 mg/L, respectively. The rate constants were calculated to be 0.026, 0.021, 0.018 and 0.016, respectively. The rate of CIP degradation was dependent on initial CIP concentration (C_0) and K_{obs} decreased as C_0 increased. The L-H kinetic model showed good agreement with the initial rates of photodegradation with an appropriate reaction rate constant and substrate adsorption constant values of $K_c = 0.245$ mg/L min and $K_{L\text{-}H} = 0.158$ L/mg, respectively.

An et al. [6] observed that CIP photodegradation followed pseudo-first-order and L-H kinetics, which is similar to the results of the current study. El-Kemary et al. [11] found that photocatalytic degradation of CIP kinetics

Table 2
Pseudo-first-order apparent constant values for the different initial concentrations of CIP

C_0 (mg/L)	R^2	K_{obs} (1/min)	Straight line equation
3	0.95	0.02	$y = 0.0266x + 0.2742$
5	0.94	0.02	$y = 0.0217x + 0.0886$
7	0.97	0.01	$y = 0.0181x + 0.1001$
9	0.99	0.01	$y = 0.0162x + 0.2125$

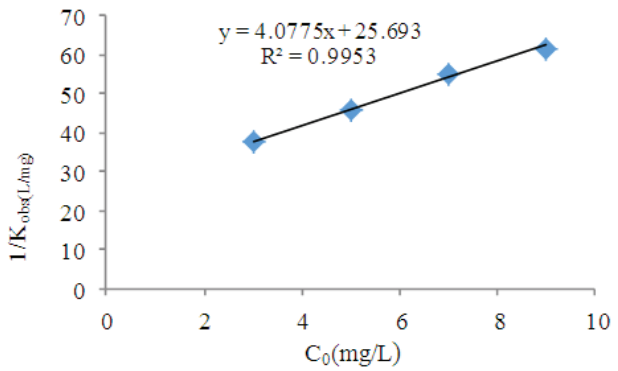

Fig. 12. Variation of reciprocal of constant rate vs. different initial concentrations of CIP.

followed a first-order reaction as well. Their results were congruent with those of the present study. According to Fig. 12, the pseudo-first-order degradation rate constant (K_{obs}) of CIP decreased when the initial concentration of CIP increased (R^2 = 0.995). This result corresponds with findings of studies by Gad-Allah et al. [33] in which it was reported that pseudo-first-order reaction rate constants for CIP photodegradation decreased as the initial concentration increased.

3.11. Thermodynamic study of CIP photocatalytic degradation

Based on the variation in the thermodynamic equilibrium constant (K_0) vs. temperature, it is possible to calculate thermodynamic functions such as changes in standard enthalpy and entropy ($\Delta H°$ and $\Delta S°$) and in the standard Gibbs free energy ($\Delta G°$).

$$K_0 = \frac{q_e}{c_e} \tag{16}$$

$$\ln K_0 = -\frac{\Delta H°}{R}\left(\frac{1}{T}\right) + \frac{\Delta S°}{R} \tag{17}$$

$$\Delta G° = -RT \ln K \tag{18}$$

In these equations, R is the general constant of gases (8.314 J/mol K) and T is the temperature (K). By using Eq. (18) and plotting the variation in $\mathrm{Ln}K_0$ against $1/T$, the change in the standard enthalpy of adsorption (adsorption heat) and the standard entropy of adsorption can be obtained from the slope and intercept of the plotted line, respectively [55]. The thermodynamic variables are provided in Table 3.

Table 3 shows that the standard enthalpy and entropy were negative. Furthermore, the Gibbs free energy increased with an increase in temperature. The negative values for $\Delta H°$ and $\Delta S°$ suggest exothermicity and diminished entropy, respectively, at the solid/liquid interface during adsorption of CIP onto the ZnO catalyst. Evaluation of the variation in the standard Gibbs free energy also indicated that adsorption of CIP onto the adsorbent was favorable at 25°C, after which an increase in temperature made the conditions of adsorption undesirable, reducing the spontaneity of the reaction.

3.12. Removal of CIP from hospital wastewater

To investigate the effect of intervening materials, experiments were carried out under optimal conditions and were repeated using hospital wastewater. The removal efficiency was then compared with the synthetic condition. The physical and chemical characteristics of the hospital wastewater are shown in Table 4.

The removal efficiency under optimum conditions (pH: 3, contact time: 90 min, ZnO immobilized on plate: 0.6 g/L, initial concentration of CIP: 3 mg/L) was 98.36% for the synthetic samples. CIP and COD removal from hospital wastewater under the optimal conditions was 90.25% and 66.66%, respectively. Intervening factors (such as TSS and COD) increased turbidity in the solution, which prevented the penetration of UV radiation and decreased the rate of photocatalytic degradation of the CIP. Competitive consumption with organic matter in real wastewater with the oxidative species and the occupation of adsorption sites on the surface of the solid catalyst appeared to decrease the degradation efficiency of CIP [56].

Table 3
Thermodynamic variables

$\Delta S°$ (J/mol)	$\Delta H°$ (kJ/mol)	$\Delta G°$ (kJ/mol)	Temperature (K)
–0.22	–75.65	–8.22	298
		–5.35	308
		–3.97	318

Table 4
Chemical and physical characteristics of hospital wastewater

Parameter	Amount
BOD_5	358 (mg/L)
COD	541 (mg/L)
TSS	261 (mg/L)
pH	7.56

4. Conclusion

This study demonstrated that immobilization of ZnO nanoparticles on glass in combination with UV radiation improved the removal efficiency of CIP. Moreover, the efficiency of removal of CIP had a direct relationship with the level of pH and reaction time and an indirect relationship with the initial concentration and the concentration of the ZnO catalyst. The maximum removal efficiency of CIP in the synthetic and hospital wastewater was 98.36% and 90.25%, respectively. This process was more stable and favorable than biological treatments and also decreased sludge production. The use of nanoparticles immobilized on glass in a photocatalytic process is a viable option for removal of the antibiotic CIP from aqueous solutions.

Acknowledgements

This paper is the result of a MS thesis carried out in the Environmental Health Engineering Research Center at Kerman University of Medical Sciences and was sponsored by the Vice Chancellor for Research and Technology of the university. The authors take this opportunity to express their gratitude for the support and assistance extended by the facilitators during the course of this research.

References

[1] A. Rhmani, J. Mehralipour, A. Shabanlo, S. Majidi, Efficiency of ciprofloxacin removal by ozonation process with calcium peroxide from aqueous solutions, J. Qazvin Univ. Med. Sci., 19 (2015) 55–64.

[2] M. Malakootian, M. Nori Sepehr, S. Bahraini, M. Zarrabi, Capacity of natural and modified zeolite with cationic surfactant in removal of antibiotic tetracycline from aqueous solutions, Koomesh, 17 (2016) 779–788.

[3] A.L. Capriotti, C. Cavaliere, S. Piovesana, R. Samperi, A. Laganà, Multiclass screening method based on solvent extraction and liquid chromatography–tandem mass spectrometry for the determination of antimicrobials and mycotoxins in egg, J. Chromatogr. A, 1268 (2012) 84–90.
[4] S. Bajpai, N. Chand, M. Mahendra, The adsorptive removal of a cationic drug from aqueous solution using poly (methacrylic acid) hydrogels, Water SA, 40 (2014) 49–56.
[5] A. Prieto, M. Möder, R. Rodil, L. Adrian, E. Marco-Urrea, Degradation of the antibiotics norfloxacin and ciprofloxacin by a white-rot fungus and identification of degradation products, Bioresour. Technol., 102 (2011) 10987–10995.
[6] T. An, H. Yang, G. Li, W. Song, W.J. Cooper, X. Nie, Kinetics and mechanism of advanced oxidation processes (AOPs) in degradation of ciprofloxacin in water, Appl. Catal., B, 94 (2010) 288–294.
[7] F. Yuan, C. Hu, X. Hu, J. Qu, M. Yang, Degradation of selected pharmaceuticals in aqueous solution with UV and UV/H_2O_2, Water Res., 43 (2009) 1766–1774.
[8] R. Darvishi Cheshmeh Soltani, A. Rezaee, M. Safari, A. Khataee, B. Karimi, Photocatalytic degradation of formaldehyde in aqueous solution using ZnO nanoparticles immobilized on glass plates, Desal. Wat. Treat., 53 (2015) 1613–1620.
[9] S.S. Kavurmaci, M. Bekbolet, Photocatalytic degradation of humic acid in the presence of montmorillonite, Appl. Clay Sci., 75 (2013) 60–66.
[10] T.H. Lim, S.D. Kim, Photocatalytic degradation of trichloroethylene over TiO_2/SiO_2 in an annulus fluidized bed reactor, Korean J. Chem. Eng., 19 (2002) 1072–1077.
[11] M. El-Kemary, H. El-Shamy, I. El-Mehasseb, Photocatalytic degradation of ciprofloxacin drug in water using ZnO nanoparticles, J. Lumin., 130 (2010) 2327–2331.
[12] M.N. Chong, B. Jin, C.W. Chow, C. Saint, Recent developments in photocatalytic water treatment technology: a review, Water Res., 44 (2010) 2997–3027.
[13] N. Daneshvar, D. Salari, A. Khataee, Photocatalytic degradation of azo dye acid red 14 in water on ZnO as an alternative catalyst to TiO_2, J. Photochem. Photobiol., A, 162 (2004) 317–322.
[14] R. Hong, J. Li, L. Chen, D. Liu, H. Li, Y. Zheng, J. Ding, Synthesis, surface modification and photocatalytic property of ZnO nanoparticles, Powder Technol., 189 (2009) 426–432.
[15] G. Huang, X. Wu, Y. Cheng, J. Shen, A. Huang, P. Chu, Fabrication and characterization of anodic ZnO nanoparticles, Appl. Phys. B, 86 (2007) 463–467.
[16] M. Janus, E. Kusiak-Nejman, A.W. Morawski, Determination of the photocatalytic activity of TiO_2 with high adsorption capacity, React. Kinet. Mech. Catal., 103 (2011) 279–288.
[17] J.R. Peralta-Videa, L. Zhao, M.L. Lopez-Moreno, G. de la Rosa, J. Hong, J.L. Gardea-Torresdey, Nanomaterials and the environment: a review for the biennium 2008–2010, J. Hazard. Mater., 186 (2011) 1–15.
[18] A. Akyol, H. Yatmaz, M. Bayramoglu, Photocatalytic decolorization of Remazol Red (RR) in aqueous ZnO suspensions, Appl. Catal., B, 54 (2004) 19–24.
[19] M.A. Behnajady, N. Modirshahla, M. Mirzamohammady, B. Vahid, B. Behnajady, Increasing photoactivity of titanium dioxide immobilized on glass plate with optimization of heat attachment method parameters, J. Hazard. Mater., 160 (2008) 508–513.
[20] A. Khataee, M.N. Pons, O. Zahraa, Photocatalytic degradation of three azo dyes using immobilized TiO_2 nanoparticles on glass plates activated by UV light irradiation: influence of dye molecular structure, J. Hazard. Mater., 168 (2009) 451–457.
[21] T. An, W. Zhang, X. Xiao, G. Sheng, J. Fu, X. Zhu, Photoelectrocatalytic degradation of quinoline with a novel three-dimensional electrode-packed bed photocatalytic reactor, J. Photochem. Photobiol. A, 161 (2004) 233–242.
[22] H.-Y. Zhu, L. Xiao, R. Jiang, G.-M. Zeng, L. Liu, Efficient decolorization of azo dye solution by visible light-induced photocatalytic process using SnO_2/ZnO heterojunction immobilized in chitosan matrix, Chem. Eng. J., 172 (2011) 746–753.
[23] H. Doan, M. Saidi, Simultaneous removal of metal ions and linear alkylbenzene sulfonate by combined electrochemical and photocatalytic process, J. Hazard. Mater., 158 (2008) 557–567.
[24] M. Malakootian, S. Dowlatshahi, M.H. Cholicheh, Reviewing the photocatalytic processes efficiency with and without hydrogen peroxide in cyanide removal from aqueous solutions, J. Mazandaran Univ. Med. Sci., 23 (2013) 69–78.
[25] M. Malakootian, M. Hashemi Cholicheh, Efficacy of photocatalytic processes using silica and zirconia nanoparticles in the bivalent nickel removal of aqueous solutions and determining the optimum removal conditions, J. Mazandaran Univ. Med. Sci., 22 (2012) 87–69.
[26] M. Malakootian, A. Mesdaghinia, S. Rezaei, The photocatalytic removal of ortho chlorophenol from aqueous solution using modified fly ash – titanium dioxide, Q. Water Wastewater, 27 (2016) 14–21.
[27] M. Fathinia, A. Khataee, M. Zarei, S. Aber, Comparative photocatalytic degradation of two dyes on immobilized TiO_2 nanoparticles: effect of dye molecular structure and response surface approach, J. Mol. Catal. A, 333 (2010) 73–84.
[28] A.D. Eaton, L.S. Clesceri, A.E. Greenberg, M.A.H. Franson, American Public Health Association, American Water Works Association, Water Environment Federation, Standard Methods for the Examination of Water and Wastewater, American Public Health Association, Washington, D.C., 1995.
[29] E. Malkoc, Y. Nuhoglu, Nickel (II) adsorption mechanism from aqueous solution by a new adsorbent waste acorn of *Quercus ithaburensis*, Environ. Prog. Sustain. Energy, 29 (2010) 297–306.
[30] A. Shafaei, M. Nikazar, M. Arami, Photocatalytic degradation of terephthalic acid using titania and zinc oxide photocatalysts: comparative study, Desalination, 252 (2010) 8–16.
[31] D.L. Ross, C.M. Riley, Aqueous solubilities of some variously substituted quinolone antimicrobials, Int. J. Pharm., 63 (1990) 237–250.
[32] D. Avisar, Y. Lester, H. Mamane, pH induced polychromatic UV treatment for the removal of a mixture of SMX, OTC and CIP from water, J. Hazard. Mater., 175 (2010) 1068–1074.
[33] T.A. Gad-Allah, M.E. Ali, M.I. Badawy, Photocatalytic oxidation of ciprofloxacin under simulated sunlight, J. Hazard. Mater., 186 (2011) 751–755.
[34] W.W. Ngah, M. Hanafiah, Adsorption of copper on rubber (*Hevea brasiliensis*) leaf powder: kinetic, equilibrium and thermodynamic studies, Biochem. Eng. J., 39 (2008) 521–530.
[35] A.Y. Shan, T.I.M. Ghazi, S.A. Rashid, Immobilisation of titanium dioxide onto supporting materials in heterogeneous photocatalysis: a review, Appl. Catal. A, 389 (2010) 1–8.
[36] S. Bekkouche, M. Bouhelassa, N.H. Salah, F. Meghlaoui, Study of adsorption of phenol on titanium oxide (TiO_2), Desalination, 166 (2004) 355–362.
[37] C.J. Wang, Z. Li, W.T. Jiang, J.-S. Jean, C.C. Liu, Cation exchange interaction between antibiotic ciprofloxacin and montmorillonite, J. Hazard. Mater., 183 (2010) 309–314.
[38] G. Crini, P.M. Badot, Application of chitosan, a natural aminopolysaccharide, for dye removal from aqueous solutions by adsorption processes using batch studies: a review of recent literature, Prog. Polym. Sci., 33 (2008) 399–447.
[39] W.T. Jiang, P.-H. Chang, Y.S. Wang, Y. Tsai, J.-S. Jean, Z. Li, K. Krukowski, Removal of ciprofloxacin from water by birnessite, J. Hazard. Mater., 250 (2013) 362–369.
[40] Y. Zhao, F. Tong, X. Gu, C. Gu, X. Wang, Y. Zhang, Insights into tetracycline adsorption onto goethite: experiments and modeling, Sci. Total Environ., 470 (2014) 19–25.
[41] M.S. Mansoury, H. Godini, G. Shams Khorramabadi, Photocatalytic removal of natural organic matter from aqueous solutions using zinc oxide nanoparticles immobilized on glass, Iran. J. Health Environ., 8 (2015) 181–190.
[42] G. Safari, M. Hoseini, H. Kamali, R. Moradirad, A. Mahvi, Photocatalytic degradation of tetracycline antibiotic from aqueous solutions using UV/TiO_2 and UV/H_2O_2/TiO_2, J. Health, 5 (2014) 203–2013.
[43] C.L. Zhang, G.L. Qiao, F. Zhao, Y. Wang, Thermodynamic and kinetic parameters of ciprofloxacin adsorption onto modified coal fly ash from aqueous solution, J. Mol. Liq., 163 (2011) 53–56.
[44] N. Caner, I. Kiran, S. Ilhan, C.F. Iscen, Isotherm and kinetic studies of Burazol Blue ED dye biosorption by dried anaerobic sludge, J. Hazard. Mater., 165 (2009) 279–284.

[45] M. Malakootian, S. Bahraini, M. Malakootian, M. Zarrabi, Removal of tetracycline antibiotic from aqueous solutions using natural and modified pumice with magnesium chloride, Adv. Environ. Biol., 10 (2016) 46–56.
[46] M. Malakootian, F. Mansuri, Hexavalent chromium removal by titanium dioxide photocatalytic reduction and the effect of phenol and humic acid on its removal efficiency, Int. J. Environ. Health Eng., 4 (2015) 19.
[47] O. Gulnaz, A. Sahmurova, S. Kama, Removal of Reactive Red 198 from aqueous solution by *Potamogeton crispus*, Chem. Eng. J., 174 (2011) 579–585.
[48] M.A. Behnajady, S. Bimeghdar, Synthesis of mesoporous NiO nanoparticles and their application in the adsorption of Cr (VI), Chem. Eng. J., 239 (2014) 105–113.
[49] H. Chen, B. Gao, H. Li, Removal of sulfamethoxazole and ciprofloxacin from aqueous solutions by graphene oxide, J. Hazard. Mater., 282 (2015) 201–207.
[50] E.S.I. El-Shafey, H. Al-Lawati, A.S. Al-Sumri, Ciprofloxacin adsorption from aqueous solution onto chemically prepared carbon from date palm leaflets, J. Environ. Sci., 24 (2012) 1579–1586.
[51] S. Khezrianjoo, H. Revanasiddappa, Langmuir-Hinshelwood kinetic expression for the photocatalytic degradation of Metanil Yellow aqueous solutions by ZnO catalyst, Chem. Sci. J., 3 (2012) 1–9.
[52] M. Malakootian, M. Pourshaban-Mazandarani, H. Hossaini, M.H. Ehrampoush, Preparation and characterization of TiO_2 incorporated 13X molecular sieves for photocatalytic removal of acetaminophen from aqueous solutions, Process. Saf. Environ. Prot., 104 (2016) 334–345.
[53] Y.S. Ho, G. McKay, Pseudo-second order model for sorption processes, Process Biochem., 34 (1999) 451–465.
[54] M. Malakootian, D. Balarak, Y. Mahdavi, S. Sadeghi, N. Amirmahani, Removal of antibiotics from wastewater by *Azolla filiculoides*: kinetic and equilibrium studies, Int. J. Anal. Pharm. Biomed. Sci., 4 (2015) 105–113.
[55] G. Moussavi, A. Alahabadi, K. Yaghmaeian, M. Eskandari, Preparation, characterization and adsorption potential of the NH_4Cl-induced activated carbon for the removal of amoxicillin antibiotic from water, Chem. Eng. J., 217 (2013) 119–128.
[56] M. Sui, S. Xing, L. Sheng, S. Huang, H. Guo, Heterogeneous catalytic ozonation of ciprofloxacin in water with carbon nanotube supported manganese oxides as catalyst, J. Hazard. Mater., 227 (2012) 227–236.